Leveraging the robustness of genetic networks: A case study on bio-inspired wireless sensor network topologies

6 **AUTHORS**, INCLUDING:

Bhanu Kishore Kamapantula
Virginia Commonwealth University
12 PUBLICATIONS **14** CITATIONS

SEE PROFILE

Preetam Ghosh
Virginia Commonwealth University
110 PUBLICATIONS **540** CITATIONS

SEE PROFILE

Michael Mayo
Engineer Research and Development Cente…
23 PUBLICATIONS **30** CITATIONS

SEE PROFILE

Edward Perkins
Engineer Research and Development Cente…
136 PUBLICATIONS **1,529** CITATIONS

SEE PROFILE

Leveraging the robustness of genetic networks: a case study on bio-inspired wireless sensor network topologies

Bhanu K. Kamapantula, Ahmed Abdelzaher, Preetam Ghosh, Michael Mayo, Edward J. Perkins & Sajal K. Das

ONLINE FIRST
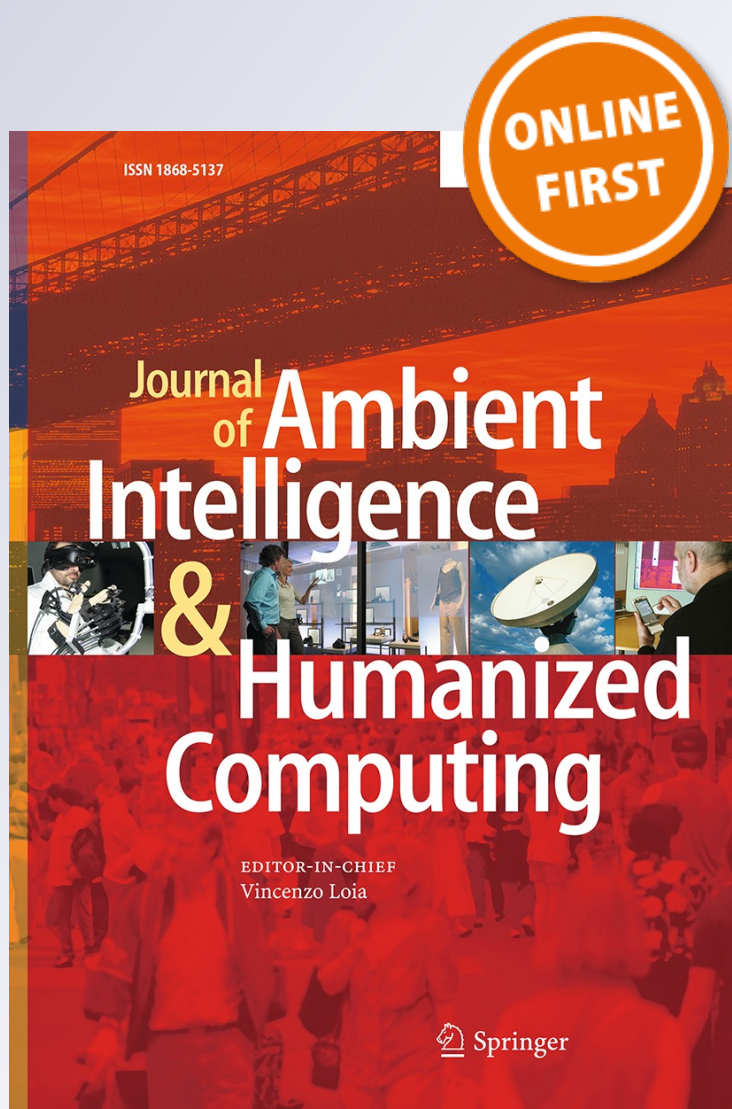
Springer

Springer

ORIGINAL RESEARCH

Leveraging the robustness of genetic networks: a case study on bio-inspired wireless sensor network topologies

**Bhanu K. Kamapantula · Ahmed Abdelzaher ·
Preetam Ghosh · Michael Mayo · Edward J. Perkins ·
Sajal K. Das**

Abstract Wireless sensor networks (WSNs) form a critical component in modern computing applications; given their size, ability to process and communicate information, and to sense stimuli, they are a promising part of the Internet of Things. However, they are also plagued by reliability and node failure problems. Here we address these problems by using the Gene Regulatory Networks (GRNs) of the organism *Escherichia coli*—believed to be robust against signaling disruptions, such as gene failures—to study the transmission properties of randomly-generated WSNs and transmission structures derived from these genetic networks. Selection of sink nodes is crucial to the performance of these networks; here we introduce four sink-node selection techniques: two motif-based, an attractor based and a highest degree-based approach and perform comprehensive simulations to assess their performance. Specifically, we use NS-2 simulations to evaluate the packet transmission robustness properties of such GRN-derived communication structures as against typical randomly deployed sensor network topologies under varying channel loss models. Packet receipt rates are compared among these networks, which are shown to be higher using GRNs for the communication structure, rather than randomly generated WSNs. We also evaluate the performance of communication structures derived from existing biological network generation models to assess their applicability in providing robust communication. This work paves the way for future development of fault-tolerant and robust WSN deployment and routing algorithms based on the inherent signal transmission robustness properties of the gene regulatory network topologies.

Keywords Gene regulatory networks ·
Wireless sensor networks · NS-2 · Robustness

B. K. Kamapantula (✉) · A. Abdelzaher · P. Ghosh
Department of Computer Science,
Virginia Commonwealth University,
Richmond, VA 23284, USA
e-mail: kamapantulbk@mymail.vcu.edu

A. Abdelzaher
e-mail: abdelzaheraf@mymail.vcu.edu

P. Ghosh
e-mail: pghosh@vcu.edu

M. Mayo · E. J. Perkins
Environmental Laboratory, US Army Engineer Research
and Development Center, Vicksburg, MS 39180, USA
e-mail: Michael.L.Mayo@usace.army.mil

E. J. Perkins
e-mail: Edward.J.Perkins@usace.army.mil

S. K. Das
Department of Computer Science and Engineering,
The University of Texas at Arlington, Arlington,
TX 76019, USA
e-mail: das@uta.edu

1 Introduction

Wireless sensor networks (WSNs) gather information from the deployed environment, which is processed and communicated to nearby nodes using a minimum of hardware: transmitters, receivers, a controller, and low-storage memory units. Large-scale WSNs are useful in military applications to monitor enemy targets, in disaster management to deliver critical environmental information, and in agricultural climate-monitoring applications. Despite these capabilities, they do not operate completely free of problems; significant issues include transmission inconsistencies, channel noise, frequent hardware maintenance, reprogramming difficulties, and node failures. These issues

increase the financial and energetic costs associated with more wide-spread implementation of such networks; reducing these costs require breakthroughs in automated maintenance and repair, more efficient energy storage and use, and a focus on reducing error and mitigating sensor and packet damage.

While much work in the physical, engineering, and computer sciences has been devoted to solving these problems, we argue here that some natural networks, when adapted to operate as communication networks, exhibit "robust" packet transmission rates under conditions of sensor failures and noisy channel characteristics, giving better performance than randomly deployed sensor nets. Specifically, we investigate how the genetic regulatory network (herein GRN) of *Escherichia coli*—a bacteria widely used as a model prokaryotic system in the life sciences—performs if "deployed" as a sensor network.

There are several parallels between genetic and sensor networks that motivate our discussions. Through a process termed transcription, genes process stimuli in the form of varying transcription factor levels—proteins responsible for activating/deactiving genes—by producing mRNA molecules directly from the nucleotide sequence of the given gene locus. These transcription products may serve as the activating factors for other genes; so, genes "communicate" with one another by processing incoming signals (varying transcription factor levels) into output signals (the mRNA) used as input for the activation/deactivation of other genes. The network mapping communication between genes in living tissues is termed the gene regulatory network.

Functional robustness of living organisms is often attributed to the optimized structures of their GRNs, which oversee the proper behavior of biological cells. A GRN designating the gene-gene interactions in cells can be modeled as a graph, where a node (representing a gene) connected to another node by an edge designates the biological processes of transcription and translation (Feng et al. 2007). The GRN topology is optimized and serves as the bio-inspiration that we seek to exploit in this paper. Although GRNs may comprise other properties (e.g., signal transmission rates or 3-dimensional organization) contributing to their robustness (none explicitly proven as yet), we restrict ourselves to only their 2-dimensional graph topologies (which denote the high-level routing topologies between genes) as they were shown to form the basis of biological robustness (Kitano 2007). Such GRNs can adapt to dynamic changes (i.e., perturbations) in the environment, and are also resilient to the removal or malfunction of nodes in the network. The signal transmission robustness of GRNs arises from their in-built redundancy and feedback control schemes and is attributed to the following: (1) Attractors: In dynamical systems, an attractor is a state which is the end-point of the system's evolution over time. In GRNs, perturbations are associated with the expression levels (or removal) of one or more genes; the dynamic behavior of GRNs is quantified by state transitions where genes are continually expressed and repressed, ultimately terminating into attractors (Kauffman 1969). (2) Motifs: specific subgraphs in GRNs are considered to be their building blocks imparting robustness (Milo et al. 2002). About 10–12 such network motifs have been identified, each consisting of 3–6 nodes. (3) Power-law degree distribution: GRNs exhibit scale-free properties due in part to their power-law degree distribution which may contribute to their robustness; such degree distribution is generated following a preferential attachment model (Albert and Barabási 2002) of adding nodes to existing GRN topologies to create GRNs of arbitrary size. Such topological properties have been identified by studying the experimentally validated GRNs from only two organisms: *E. coli* and yeast; the GRNs of most other organisms have not been identified or validated as yet.

Similarly, wireless sensor networks (herein WSNs) are nets of communicating sensor motes, whereby hardware is responsible for processing incoming signals (the packets) into outgoing messages (packet forwarding). Since living cells are able to adapt to disruptions to the genetic "signals" due, in part, to the evolved network architecture, we hypothesize that a deployed sensor network architecture based upon GRN topology will adopt similar "robust" signal-transmission properties.

Adaptive routing schemes have been well studied in WSNs, with respect to resilience against channel errors, node failures or congestion (Li and Mohapatra 2007). Some current MAC protocols ensure reliable multi-hop data forwarding; however, NS2-based simulations revealed that IEEE 802.15.4 possess very low packet-transmission reliability with power management enabled for energy conservation (Anastasi et al. 2010). Other routing schemes serve as transport protocols in WSNs (Wang et al. 2006), while experimental validation strategies are enforced to improve the reliability (Kim et al. 2004; Woo et al. 2003). Validation in the Motes (Tiny 2009) and Sunspot (Sun Microsystems 2009) is supported by link-quality estimation schemes that evaluate the stability and reliability of routes (Couto et al. 2003; Fonseca et al. 2007), and locate alternate routes when some sensors fail (Gnawali et al. 2009). In this paper, we present a mapping between gene regulatory networks and wireless sensor networks to motivate the design of sparse yet robust communication structures and hence, signal routing schemes in WSNs and perform comprehensive NS-2 (McCanne and Floyd 1997) based simulations to assess the feasibility and benefits of our approach.

The paper is organized as follows. Section 2 discusses the notion of biological robustness as observed in their gene regulatory networks. Section 3 explains our gene-sensor mapping rules to derive sparse bio-inspired communication structures that can improve the WSN packet-transmission characteristics. To evaluate our approach, we first discuss the generation of random and biological network models (Sect. 4). To simulate transport of packets between two distal regions of the network requires the

identification of "sink" nodes, i.e. nodes that receive packets, but do not forward them to others. To this end, three sink selection methods are proposed and evaluated in Sect. 5 while the packet transmission characteristics of such GRN-derived networks were discussed in Sects. 6, 7 discusses the limitations of existing biological topology generation algorithms in creating such smart communication structures in WSNs. Finally, the implications of this work are discussed in the context of future work in the sensor network field (Sect. 8). These results extend those reported in (Kamapantula et al. 2012).

2 Robustness in GRNs: the notion of attractors

We will first explain the theoretical basis of biological robustness as seen in the GRNs using mathematical models of the signal transmission state space. These models will subsequently be used in one of our proposed sink selection strategies in GRN-based communication structures.

If the genes of an interacting network occupy one of only two possible states (ON or OFF), and if transitions may occur between the corresponding network states by selective gene activation/deactivation (ON or OFF and vice versa), then the network state in the long-time limit is called an attractor (Kauffman 1969). In general, there can be many attractors for a given network, and it may cycle through some of them indefinitely. The network's state-transition diagram is partitioned into level sets l_j, that include all of the states that terminate with an attractor state in exactly j transitions. Such attractor cycles are mutually disjoint, and the partition class corresponding to an attractor cycle is called the basin of the cycle, with any transient state belonging to a unique basin and level.

The dynamical behavior of a GRN can be represented by its state transitions-along with some degree of fault-tolerance-in which its genes are continually expressed and repressed, and ultimately terminate with attractors and cycles. To quantify these states, two formalisms have been proposed: Boolean and Probabilistic Boolean networks.

2.1 Boolean networks

Boolean network (BN) models were first introduced to study the expression patterns of randomly constructed "genetic nets" (Kauffman 1969). In a BN, a gene can be in either of two possible states, ON/OFF, where the state (or expression level) of each gene is functionally related to that of other genes using logical rules, or "functions". A BN is defined by a set of nodes, $V = \{x_1, x_2, \ldots, x_N\}$, corresponding to a set of genes, together with a list of Boolean functions $F = \{f_1, f_2, \ldots, f_N\}$, one for each node, that determine the node-node interactions. The state of the entire network is labeled in the form $x_1 x_2 \ldots x_N$ (e.g. $010 \ldots 1$), wherein the individual gene-states are either 1 (ON) or 0 (OFF). Transitions between them are triggered by adjusting a gene's state, and are represented by a directed graph (Fig. 1a).
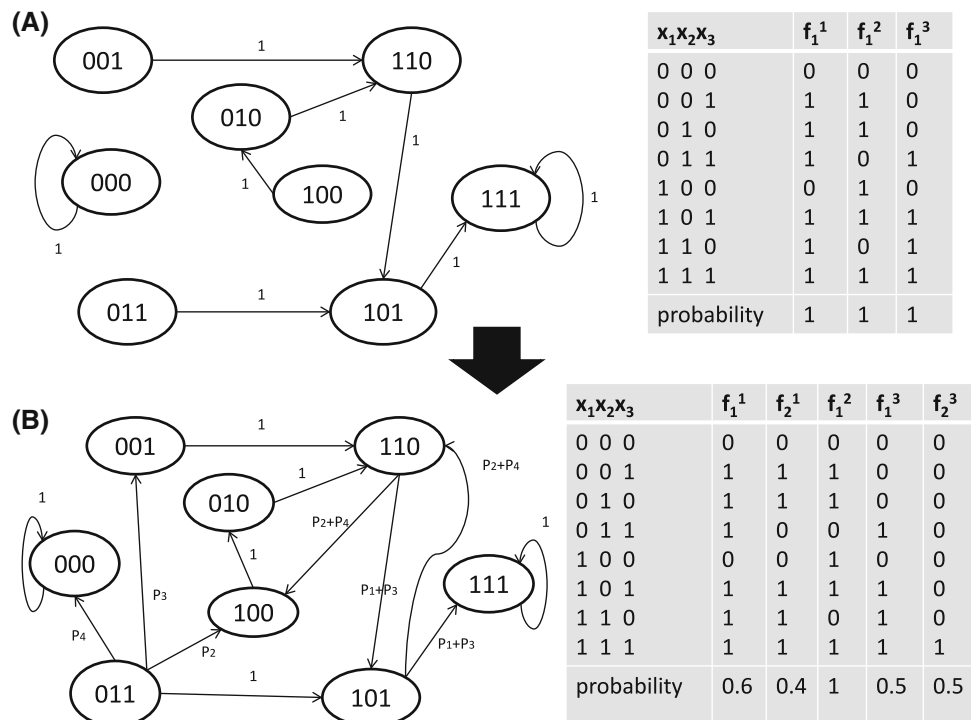

$x_1 x_2 x_3$	f_1^1	f_1^2	f_1^3
0 0 0	0	0	0
0 0 1	1	1	0
0 1 0	1	1	0
0 1 1	1	0	1
1 0 0	0	1	0
1 0 1	1	1	1
1 1 0	1	0	1
1 1 1	1	1	1
probability	1	1	1

$x_1 x_2 x_3$	f_1^1	f_2^1	f_1^2	f_1^3	f_2^3
0 0 0	0	0	0	0	0
0 0 1	1	1	1	0	0
0 1 0	1	1	1	0	0
0 1 1	1	0	0	1	0
1 0 0	0	0	1	0	0
1 0 1	1	1	1	1	0
1 1 0	1	1	0	1	0
1 1 1	1	1	1	1	1
probability	0.6	0.4	1	0.5	0.5

Fig. 1 BN vs PBN dynamics for GRNs. The attractor nodes are 000 and 111 in both cases. The *truth tables* for the BN and PBN are shown alongside

As an example, consider a Boolean network with only three genes: $V = \{x_1, x_2, x_3\}$ wherein a Boolean function is associated to each of them according to the truth table shown in Fig. 1a. Out of potentially $2^3 = 8$ attractors, this BN has exactly two: 000 and 111. Here, a single Boolean function describes the next state of any gene based upon the wiring rules of the corresponding GRN; the probability to choose these particular functions is always 1.

2.2 Probabilistic Boolean networks

The Probabilistic Boolean network (PBN) formalism was developed out of the need for a network to cope with uncertainty; one challenge is to identify the correct regulatory relationships for a target gene (Shmulevich et al. 2002), while also preserving the rule-based properties of BNs.

More specifically, PBNs accommodate more than one possible function for each node in the network. A set of functions $F_i = \{f_j^i : j = 1, 2, \ldots, l_i\}$ is associated with each gene x_i, where each function associated to a given gene, f_j^i, determines the expression value x_i of that gene, and l_i is the number of possible functions for that particular gene. In Fig. 1b, the values for the first and third gene, x_1 and x_3, are, respectively, determined by two possible functions; i.e., f_1^1 and f_2^1 for x_1 (with others similarly described).

A realization of the PBN at any given instant is determined by a vector of Boolean functions, where the *ith* element of the vector contains the predictor selected for the gene x_i. This vector function maps one network state onto another, and is referred to as a multiple-output Boolean function. Since each of the N possible realizations (for N genes) is a standard BN, valid for only one time step, a PBN describes the evolution of an ensemble of alternative BN states for each gene. The probability for the *ith* BN to be selected is written in terms of the individual selection probabilities, shown in the bottom row of the truth table within Fig. 1b [see (Shmulevich et al. 2002) for further details].

3 Gene-sensor mapping rules

Transmission inconsistencies often plague WSNs where they suffer from signal disruptions due to sensor failure, or from the absence of routing protocols that are sufficiently insensitive to local as well as global network conditions. As GRNs are subject to operating conditions conceptually similar to WSNs, the evolution of their attractor state-space can be equivalently described within a WSN context according to the following rule (Ghosh et al. 2011): (1) for every gene within the GRN, we replace it with a sensor; (2) sensor interactions are restricted to existing edges between corresponding genes in the GRN. In the following sections, we discuss the implications of these gene-to-sensor mapping rules to WSN packet-transmission characteristics.

3.1 Packet transmission along wireless channels

Rule one states that the GRN node structure is preserved in WSN. Rule 2 defines the interactions between sensors in terms of packet transmission, with respect to the GRN architecture. According to the second rule, a sensor (or equivalently, a gene) at time interval t can either send or not send a packet to another sensor—one that either promotes or suppresses another gene—at time interval $t+1$ with a certain probability (as a function of the network state, packet error rate or the distance between corresponding sensors) and destination node break-down probability. Thus, a gene is considered to be either in state *1* or *0*, based on whether it is up-regulated or down-regulated. Similarly, a sensor will be in states *1/0* depending on whether it has received a packet or not.

3.2 Wireless sensor topology

The physical signaling structure of sensors within the WSN must be adapted to reflect the interplay between genes in the GRN. If gene G_1 up-regulates G_2, then the equivalent interaction in the WSN is that sensor G_1 sends a packet to G_2 according to specific probability distribution defined by gene–gene interactions. For homogeneous sensor nodes, each up-regulation edge (denoted by $+$) in a GRN is replaced by a bi-directional edge; if we allow sensor G_1 to send a packet to G_2, then G_2 should also be able to send a packet to G_1 (see Fig. 2b). For heterogeneous sensor nodes, however, it is not necessary that both G_1 and G_2 possess the same transmission radii, giving a directed edge from G_1 to G_2 and not vice versa (such a network is shown in Fig. 2c).

3.3 Packet collisions

According to the second rule, biological down-regulation must also be mapped from a GRN to a WSN. If G_1 down-regulates G_2, then sensor G_1 prohibits the receipt of packets at sensor G_2. This phenomenon is interpreted as packet "collisions" in the WSN; data packets simultaneously received by G_2 from both G_1 and G_3 result in effectively zero packets received by G_2.

3.4 Attractors and packet transmission scenarios

Using the BN formalism, each attractor will record the transmission history of the packet. Figure 1a depicts two attractor states of an exemplary BN—000 and 111. Here, the evolution of the initial state 001 to an attractor is analogous to one in which gene x_3 transmits a signal to its neighbors; the
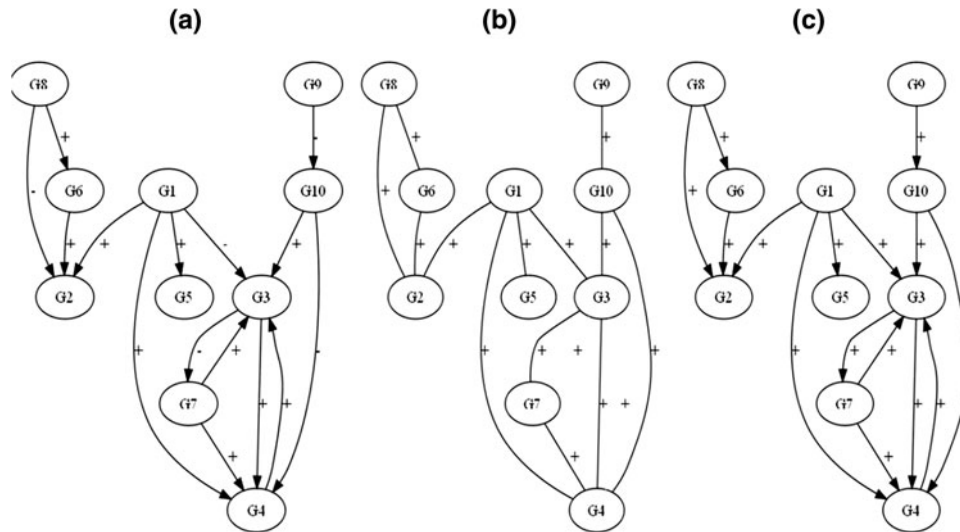
Fig. 2 Schematic of GRNs (extracted from GeneNetWeaver), and their equivalent WSNs: **a** A 10-node GRN from the yeast cell cycle; **b** Equivalent 10-node WSN from (**a**) where each edge is undirected as two sensor nodes within transmission radius of each other (assuming homogeneous nodes) can send packets to each other and there is no down-regulation involved; **c** Restricted WSN from (**a**) with no down-regulation and an edge from G_i to G_j does not imply the existence of an edge between G_j to G_i. This network abstracts the case for heterogeneous sensors and also the scenario of dynamic routing where a sensor only transmits packets along its outgoing edges although it is capable of sending packets back to the transmitting nodes (incoming edges)

network then evolves according to a sequence of state-transitions until it terminates in attractor 111. Ultimately, all three genes x_1, x_2 and x_3 of Fig. 1a will receive a signal originating from gene x_3. Similarly, if gene x_2 receives a signal from all the other ones (equivalent to setting node x_2 as the Cluster Head in the WSN), then each of the three initial states of 001, 010 and 100 will ultimately reach the attractor 111 in 3, 3 and 4 state transitions, respectively.

The PBN formulation reproduces the attractors 000 and 111 of this 3-node system, shown in Fig. 1b. The PBN formalism allows us to incorporate the packet-drop rates due to "noisy" channel characteristics into the packet transmission state-space by redefining the perturbation probability from (Shmulevich et al. 2002) for each edge in the WSN.

4 Generating model networks

In this paper, we will primarily be comparing the performance of the GRN-derived WSN topologies with random wireless sensor networks (RWSNs). Such RWSNs are the standard models for WSN topologies wherein the resulting communication structure, taken as the networks' transmission skeleton, is conceptually equivalent to an Erdös-Renyi random graph. The RWSNs serve as the benchmark networks in this study and were generated as follows.

A WSN module in the Python programming language (Foundation 1991) is used to generate these models. Here, two different nodes within the network are chosen at random, and a link is established between them with probability p. Networks with 100, 150, 200, 250 and 300 nodes were generated for demonstration purposes as representing "medium" sized sensor networks. 25 networks of each size (100, 150, 200, 250 and 300 nodes) are considered to illustrate the sink node selection approach. Networks of a certain size are spread over an area with specific node transmission range. For example, 25 different networks of size 150 nodes are spread over 3.6×10^5 m^2 (with x = 600 m and y = 600 m) with a node transmission range of 85 m. Node range for a network has been assigned based on the work by (Han et al. 2009). Similarly, networks of size 200 are spread over area of 4.9×10^5 m^2 (with x = 700 m and y = 700 m) with a node transmission range of 90 m and networks of size 250 are spread over 8.1×10^5 m^2 (with x = 900 m and y = 900 m) with a node transmission range of 90 m. Networks of size 300 are spread over an area of 10^6 m^2 (with x = 1,000 m and y = 1,000 m) with a node transmission range of 110 m. Each of these networks of particular size are compared to the respective GRN-derived network of the same size, the results of which are reported in Figs. 14 and 15. The following algorithm describes the procedure to add edges in a RWSN.

Algorithm Algorithm to add edges in RWSN

---

for S network size **do**
   For s in nodes
   remove s from destinations
   if $euclidean\_distance(s, dest)$ $<=$ $transmission\_range$ **then**
     add an edge between source and dest
   end if
end for

An entirely different type of network is represented by the gene regulatory network of *E. coli*, wherein the probability to find a node of degree k, $p(k)$, follows a power-law $p(k) \sim k^{-\gamma}$, wherein $\gamma = 2.1 \pm 0.3$ (Vázquez et al. 2004)—although, new research restricts all realizable scale-free networks to $\gamma \geq 2$ (Genio et al. 2011). Model GRNs of varying size are generated using the Gene-NetWeaver tool, originally presented as a platform to test the capability of differing gene network inference algorithms (Schaffter et al. 2011), providing directed sub-networks of user-defined size from the full *E. coli* transcriptional network. For simplicity, we ignore the direction of links between genes resulting from Gene-NetWeaver, and no directionality is assigned to the edges (this correspond to the mapping depicted in Fig. 2c); the implications of directed graphs on the WSN transmission characteristics will be considered elsewhere.

4.1 Matching criterion to compare GRNs and RWSNs

All scale-free networks are sparse (Genio et al. 2011), and many biological networks, including the genetic network of *E. coli*, are scale-free. This is quite different from randomly generated networks, wherein their degrees are Poisson-distributed. For a meaningful comparison between RWSN and GRN models, we ensure the following characteristics in both type of networks:

1. Use same number of nodes (N) and edges in both GRN and RWSN
2. Use same simulation characteristics, such as packet transmission rate and link bandwidth, for both GRN and RWSN as mentioned in SubSect. 4.2.
3. Ensure no self-edges (Example: For node a, a → a is a self edge) for any node in the considered GRNs and RWSNs

If a RWSN contains more number of edges after network generation, edges are deleted to match the edge count in GRN-derived network. For this process, two nodes are randomly selected and checked if they share an edge in the RWSN. That edge is deleted if it exists. Edges are not deleted from a node if its edge count falls below two (after deletion). If an edge deletion disconnects the network, that edge is added back thus ensuring network connectivity.

To utilize these generated model networks for packet-transmission scenarios, a source and sink/receptor node must be specified; transmission originates with the source node(s), and terminates at the sink. The choice of a sink node is important in the context of providing robustness in the GRN derived WSNs and we will propose and evaluate several sink selection strategies in the next section.

GeneNetWeaver does not generate multiple GRNs with same number of edges for given network size. However, we could process the imbalanced (in terms of matching the edge count) networks by deleting or adding the edges. But by doing this we lose the inherent structural advantages of a GRN. Hence, we evaluate the performance of 25 RWSNs against one GRN of a particular size.

4.2 NS-2 implementation

Transmission scenarios were evaluated using NS-2 simulations. A duplex-link is established between the nodes (based on input files) that have edges in RWSNs/GRNs. A bandwidth of 1 Mb is assigned for each link in this simulation, with a packet interval of 1 ms. Ten simulations are executed for every category of observation using a flooding routing protocol. Information is transmitted at periodic intervals and the packet receipt rate at the sink node is recorded. A packet-loss model is used to evaluate the performance of each network of fixed size, in which packet-loss of 1–20 % is considered. Different packet sizes are used in each of the ten simulations as follows: 900, 15, 444, 333, 334, 335, 31, 337, 338 and 339 bytes respectively. Hence, the reported results show the average delay performances by considering variable packet sizes to some extent. A more detailed analysis of how packet size affects the delay in such GRN-derived networks will be addressed in the future.

5 Selecting sink nodes

Sink node selection is critical to the implementation of NS-2 simulations that model packet-transport across the sensor network. One method to choose such nodes in the scale-free *E. coli* genetic network is to appeal to its topological structure. A power-law degree distribution in the *E. coli* network (independent of link directionality), $p(k) \sim k^{-\gamma}$, ensures that very few nodes have large numbers of nearest neighbors, $\lim_{k \to \infty} p(k) = 0$, but also guarantees most nodes are of low degree, $\lim_{k \to 1} p(k) = 1$. Nodes with drastically larger numbers of nearest neighbors than the average are termed "hubs" (Albert and Barabási 2002); their strong coupling to the rest of the network implies they have a greater chance of participating in paths connecting opposing sites of the network, making them a natural choice for the sink node. This scheme is termed Highest Degree, or HD.

Another scheme for sink-node selection is based on the observation that gene regulatory networks are composed of repeating elementary substructures that serve specific functions, termed motifs (Milo et al. 2002). Various types of motifs have been identified previously in biological networks, and Fig. 3 displays all 13 possible connected 3-node motifs. Three node motifs, specifically the most frequently observed feedforward loop (herein FFL), play a

Fig. 3 Types of three-node motifs
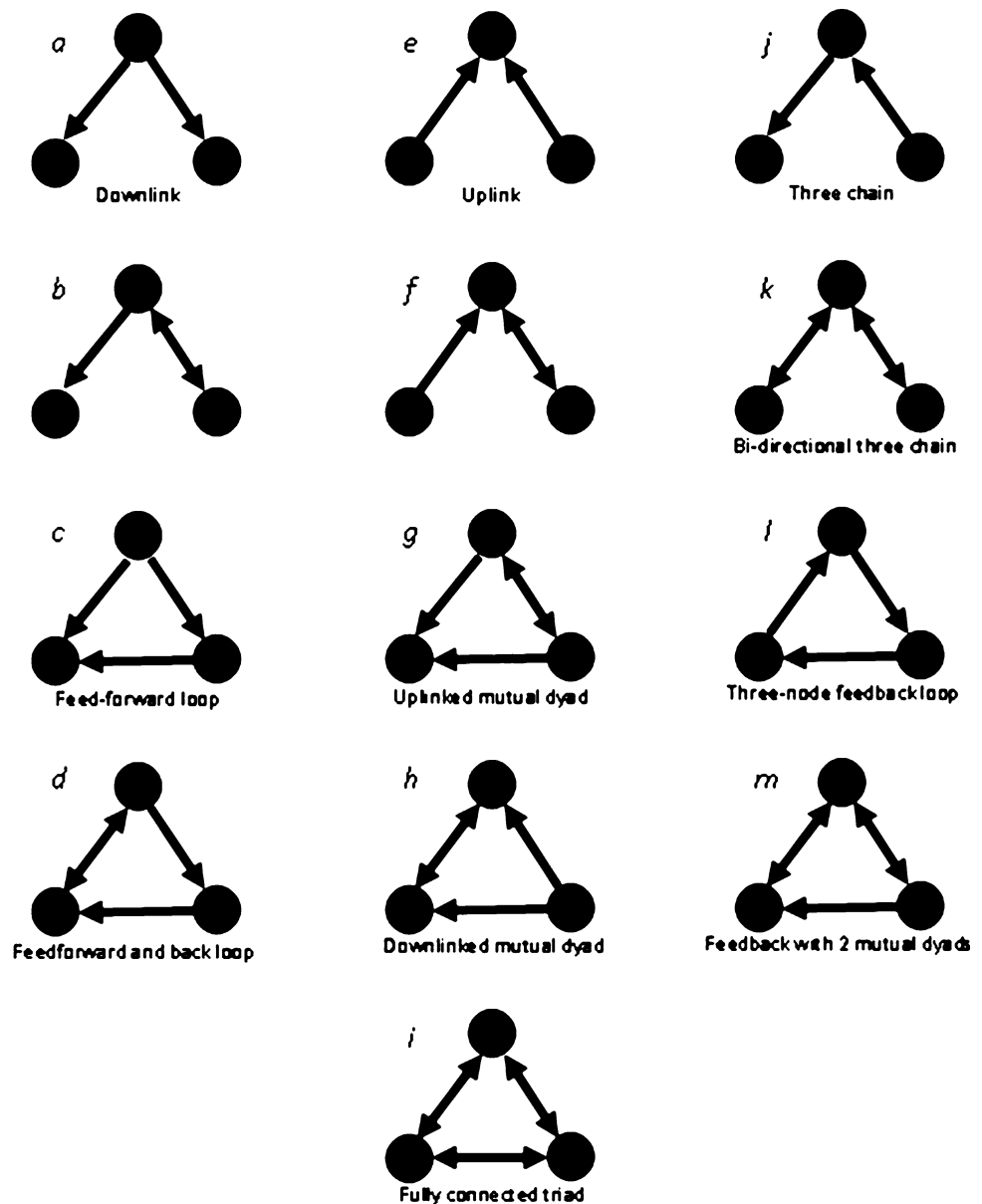
critical role in establishing robustness—the ability of a system to preserve its *function* despite external or internal perturbing influences (Kitano 2007)—in genetic networks. Moreover, the FFL is known to support critical functions, such as irreversibly speed up or delay response times in target genes, or generate signal pulses (Mangan and Alon 2003). The occurrence of the most abundant motifs in *E. coli* is presented in Table 1. Based on this evidence, we hypothesize that a sensor node most frequently involved in a FFL in the network's communication structure is a superior choice of sink node for the transmission scenarios under study here. This scheme is termed the motif-based approach, or MB.

In addition to the MB method, a more general method in which a node is involved in *any* 3-node motif is termed highest-coverage method, or HC.

5.1 Identification of sink nodes in GRN-derived networks

We compared the HC, HD, and MB methods, which is tabulated in Table 1. Nodes maintain their identifying labels between all model networks, and nodes identified using the highest motif coverage (HC) method (represented in 2nd column) are **boldened**. Similarly, nodes identified using the highest degree (HD) method (represented in 3rd column) are **boldened**. Finally, nodes represented by braces, {}, indicate the labeled nodes have either the same degree or the same feed-forward loop coverage using the MB method. In each comparison, the node boldened can be considered as the sink node for that particular network.

Table 1 Abundance of motifs in *E. coli* genetic networks

Name	Symbol	Abundance
Feed-forward loop		1,860
Uplinked mutual dyad		878
Downlinked mutual dyad		34
Three node feed-back loop		12
Feed-forward and -back loop		10
Feed-back with two mutual dyads		8
Fully connected triad		3

Table 2 Sink node selection in the GRN-derived networks: motif— and highest degree-based methods

Network size	Nodes with 1st, 2nd, 3rd HC in that order	Nodes with 1st, 2nd, 3rd HD in that order	MB
20	**3**, 2, 1	**3**, {1, 2}, 8	3
25	**1**, 13, 3	**1**, {13, 14} 3	1
30	**14**, 1, 8	**14**, {1, 8}, 4	{1, 14}
35	**2**, 29, 22	**2**, 29, 22	N/A
40	**12**, 16, 15	**12**, 16, 15	{12, 16}
45	**14**, 18, 17	{**3**, **14**}, 18, 13	{14, 187}
50	**3**, 16, 19	**3**, 16, 19	3

Table 3 Sink nodes chosen using the highest degree, or HD, method for GRN-derived model networks of varying size

Network size	Degree of selected node
100	70
150	127
200	97
250	146
300	135

Because we observed that nodes with highest degree also qualify as nodes with highest motif coverage (using both methods of motif coverage, HC and MB), from hereon

we disregard the other methods described above, using only those nodes identified as sink nodes using the HD method for the GRN-derived modeled networks. Although this equivalence between nodes identified across all methods is intuitive—i.e., hubs are strongly connected to the rest of the network, participating in the most sub-networks—we should emphasize that further experimentation, either by numerics or analytical methods, are required to establish this observation beyond all doubt. The chosen sink nodes based on this method are reported in Tables 2, 3 that were used to generate the results in the next section.

5.2 Emphasize highest degree approach as sink node selection for GRNs

In order to establish the selection of sink nodes in our GRN-derived WSNs using the highest degree approach, extensive simulations were performed. Five different 20 node GRN derived networks were generated first using GeneNetWeaver. Figures 4, 5, 6, 7, 8 present the percentage of packets received using three different approaches to select sink nodes across these five networks. The abbreviations used for labeling the sink nodes from each scheme are summarized in Table 4: (1) MB refers to nodes having highest motif coverage as discussed earlier; (2) FHD, SHD and THD are respectively the nodes having highest, second highest and third highest degrees and all belong to the HD category of sink node selection as discussed before; (3) a PBN based sink node selection scheme. Note that the first two sink node selection approaches were discussed previously in the context of larger GRN-derived networks and we observed that the FHD approach recorded the best performance in most cases. The simulations also considered the second-highest and third-highest degree nodes as candidate sinks as these cases produced slightly better successful packet receipt rates for networks 1 and 3 (Figs. 4, 6) under higher simulated channel error conditions. Note that the terminology (x,y) is used in these figures to designate cases where the same node was picked to be the sink under x and y schemes. This points to an important observation: the highest degree node by itself may not serve as the best candidate for the sink under higher channel errors; instead, all nodes having higher degree (than the average degree) need to be evaluated as they work together in providing packet transmission robustness. This observation follows the established protocol in biological networks wherein robustness is mainly conferred by the number of hub nodes (that correspond to the higher degree nodes) and not simply by the largest hub node in the network. It might be beneficial to consider multiple local sinks (based on the number of hub nodes) in such cases to provide higher network robustness in our GRN-derived sensor network formulation.

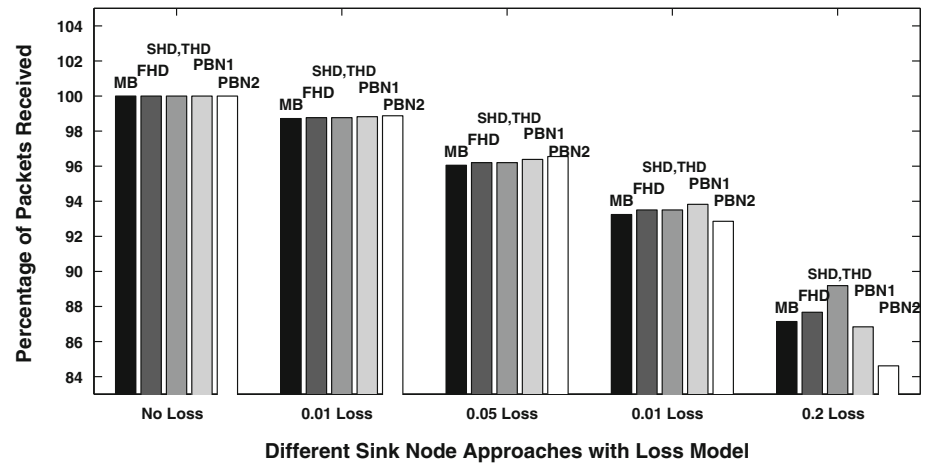**Fig. 4** Sink node selection and respective packet received percentages with Loss Model—1st 20-node GRN

Fig. 5 Sink node selection and respective packet received percentages with Loss Model—2nd 20-node GRN
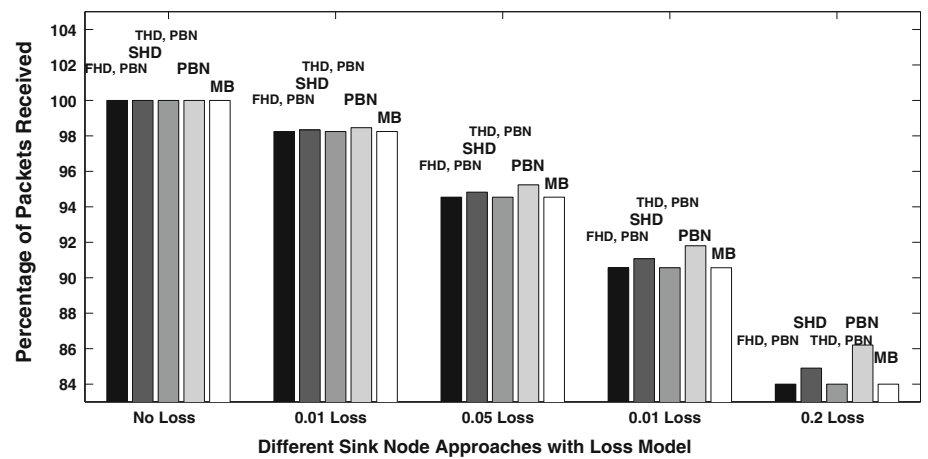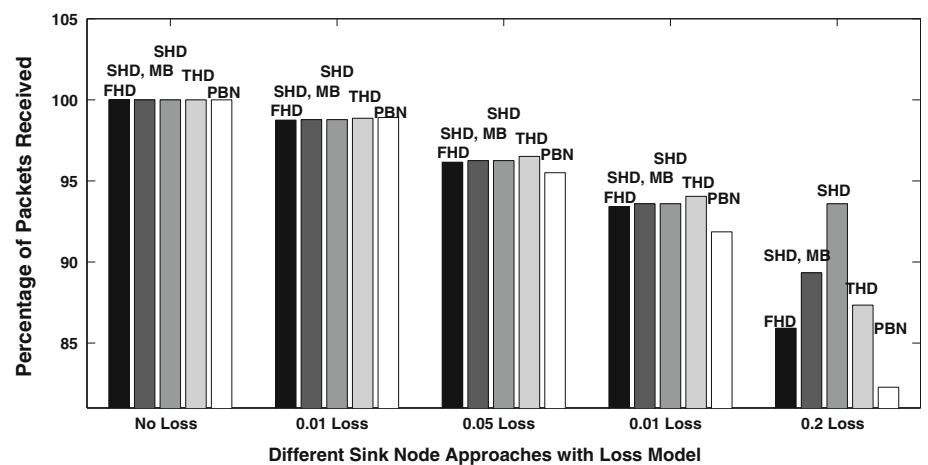

Fig. 6 Sink node selection and respective packet received percentages with Loss Model—3rd 20-node GRN

The third sink node selection scheme is directly related to the biological model for robustness in terms of the attractor states as defined before and needs some explanation. Recall that an attractor in a 20-node GRN derived network is a boolean bit-string of length 20; for example,

Table 5 shows a schematic with 5 different attractor states generated using the PBN model for a particular 20-node GRN-derived network. Here, each bit, S_i denotes whether the corresponding sensor has received the packet in the long time limit that originated from other sensors. Ideally, a

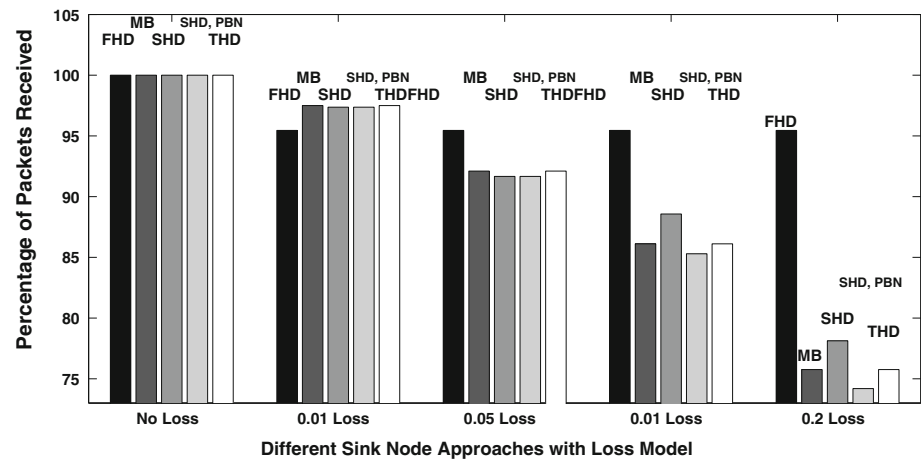**Fig. 7** Sink node selection and respective packet received percentages with Loss Model—4th 20-node GRN

Fig. 8 Sink node selection and respective packet received percentages with Loss Model—5th 20-node GRN
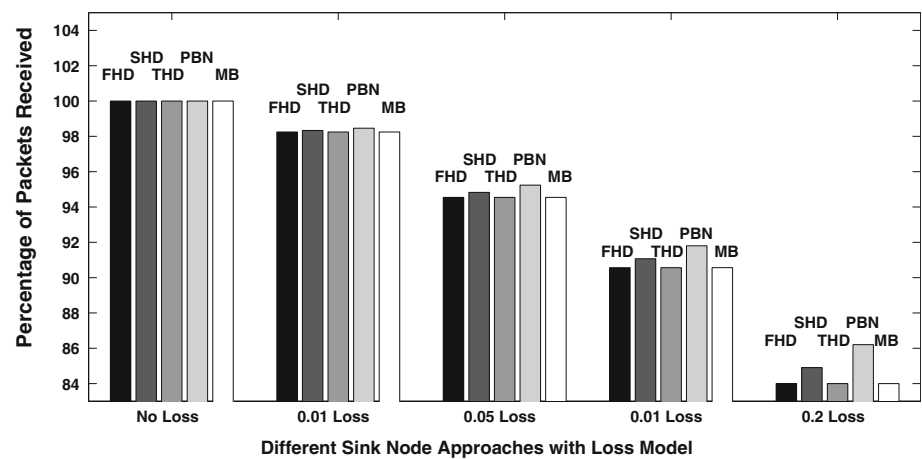

Table 4 Sink node selection approach and Description of its abbreviated forms for Figs. 4, 5, 6, 7, and 8

Selection approach	Description
MB	Node with highest motif coverage as sink
FHD	Node with first highest degree as sink
SHD	Node with second highest degree as sink
THD	Node with third highest degree as sink
PBN	Node selected using the PBN approach as sink

sink node should be chosen as that sensor which receives the maximum number of packets; hence, considering the attractors to be the long-term limits of the packet transmission state-space, the sum of the bits in each column from its attractor states signify how likely it is for this particular sensor to receive a packet passed around in the network. In this example, sensor S_{11} has the highest column sum and can be considered as the best candidate for the sink node. The PBN based selection scheme identifies the sink nodes using this methodology (PBN1 and PBN2 in Fig. 4 identifies the top two nodes respectively having the

highest and second-highest column sums). Figure 4 shows PBN1 gives better performance than PBN2 in terms of packet receival rates; we have observed this trend to be consistent across all GRN-derived networks and hence only reported the results of PBN1 in Figs. 5, 6, 7, and 8 (labeled simply as PBN in the figures). Multiple representations of PBN in one figure (example Fig. 5) mean that multiple sinks have been identified by PBN-based scheme. It can be observed that the HD approach show comparable performance than when compared to the PBN-based sink selection schemes.

Note that these separate set of simulations were intentionally conducted on smaller GRN-derived networks (with 20 nodes) as the PBN-based models have severe computational overhead and generally fail to work for networks of size ≥ 30 nodes. Although the PBN based scheme seem to work better in most cases, it may not be feasible to compute for larger networks. This points to the importance of the HD approach in selecting sink nodes to achieve high packet transmission robustness in the GRN-derived networks.

Table 5 Sink node selection using probabilistic Boolean network (PBN) approach

PBN state	S1	S2	S3	S4	S5	S6	S7	S8	S9	S10	S11	S12	S13	S14	S15	S16	S17	S18	S19	S20
Attractor 1	1	0	1	0	1	0	0	0	1	0	1	0	1	0	0	0	1	0	1	0
Attractor 2	1	0	1	0	1	0	1	0	0	0	1	0	1	0	1	0	1	0	0	1
Attractor 3	1	1	0	0	1	1	1	0	1	0	1	0	0	0	1	1	1	1	0	1
Attractor 4	0	0	1	0	1	1	0	0	1	0	1	1	0	0	1	0	1	0	1	0
Attractor 5	0	0	0	1	0	0	1	0	1	1	1	0	0	0	0	1	0	0	1	0
Sum	3	1	2	1	4	2	3	0	4	1	**5**	1	2	0	3	2	4	1	3	2

Table 6 Sink node selection—random WSN

Network size	Number generated as sink node	Packets received (%)	
100	5, 0, 31, 18, 98, 90, 14, 35, 57, **99**, *68*	49.8947, 49.896, 49.4781, 50.3132, 50.4167, *49.152542,*	50.8403, 50.5219, 49.8956, 50.5219, **51.2712,**
150	115, **136**, 80, 8, 32, 19, 116, 57, 145, 13, *149*	50, 49.812030, 50, 50.187265, 50.187265, *51.190476,*	**50.282485,** 49.812734, 49.717514, 49.718574, 50,
200	58, 36, 50, 1, 83, 55, 88, 23, 47, **11**, *199*	49.938195, 49.752475, 49.783549, 49.783549, 50, 49.907235, *50.031948,*	50, 49.938195, 50, 50, **50.248138,**
250	217, 42, 99, 184, 197, **104**, 166, 85, 73, 22, *249*	49.958506, 50.124069, 50, 50.082644, 49.792874, *48.970840,*	49.875724, 50.124069, **50.207125,** 49.834437, 49.917081,
300	111, 67, 158, 283, 71, 34, **17**, 210, *299*, 249, 221	50.137849, 50.019646, 49.960691, **50.157604,** *49.478748,* 49.960629,	49.763593, 49.921197, 49.822485, 50.039277, 49.941060,

5.3 Identification of sink nodes in RWSNs

We first report the packet receival characteristics of GRN derived networks and RWSNs using the same criterion (i.e., the HlD method) for selecting the sink node. Figure 9 illustrates that GRN derived networks are more robust than RWSNs with this criteria under varying network size.

In RWSNs, sink nodes are generally chosen at random. Here, a random number is generated from 1 to N, where N = 100, 150, 200, 250, or 300 is the number of nodes in the model network. Ten random numbers were generated for each model network; given that each node of the network is labeled $i = 1, \ldots, N$, these random numbers select nodes that are each considered to be a sink. Next, separate simulations were conducted with each of these choices for sink nodes and the packet receival rates were observed. The results have been reported in Table 6. Note that, sink nodes 99, 136, 11, 104, 17 perform best (highest packet receival rate) for the 100, 150, 200, 250 and 300 node networks respectively. However, nodes 68, 149, 199, 249, 299 have the highest degree for 100, 150, 200, 250 and 300 node RWSNs respectively. These nodes (with highest degree) and the corresponding packet receival rates when they are chosen as sinks are *italicized*; whereas, the nodes giving best performance when selected as sinks and their corresponding packet receival rates are **boldened** in Table 6. This illustrates the fact that nodes with highest degree are not necessarily the best choices for sink nodes in RWSNs. The best performing sink nodes amongst the 10 options considered (the results in bold), will be used in the next section for performance comparison with GRN derived networks.

6 Results

Hereafter, GRN-derived sensor networks are termed as GRNs in figures for convenience.

6.1 GRN-derived model networks improve transmission reliability

Using NS-2 simulations, we find the ratio; N/N_0, of packets received at the aforementioned sink nodes, N, to the total number of packets sent from the source, N_0, and is consistently higher in the sensor networks derived from the
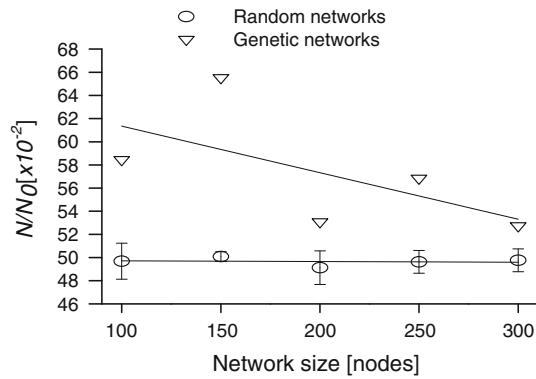
Fig. 9 The fraction of sent packets arriving at the sink, N/N_0, is measured using the Highest Degree (HD) method in GRN-derived sensor networks. Sinks are chosen at random in the random wireless sensor networks (RWSNs)
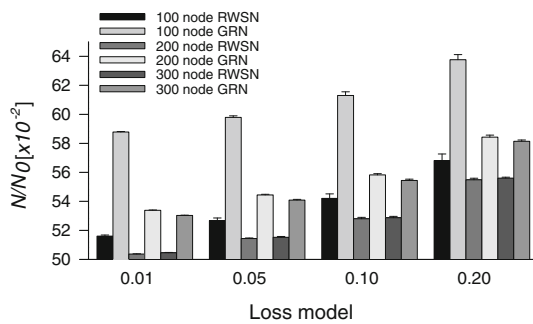

Fig. 10 Fraction of successful packet transmissions, N/N_0, as measured across GRN-derived and random sensor networks of varying size under differing loss models
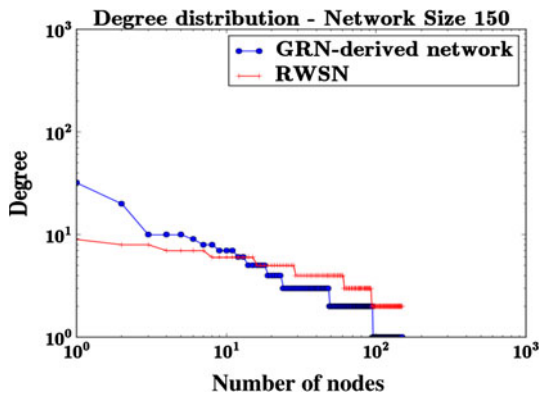

Fig. 11 Degree distribution of GRN-derived sensor networks, RWSNs—Network size 150

E. coli transcription network than the random wireless networks as illustrated in Figs. 9, 10, 12. This result holds for all simulated packet loss scenarios: (1) with no packet loss model implemented (reported in Fig. 9), (2) with loss model ranging from 0.01 to 0.2 wherein 1–20 % of transmitted packets were "lost" (reported in Fig. 10).
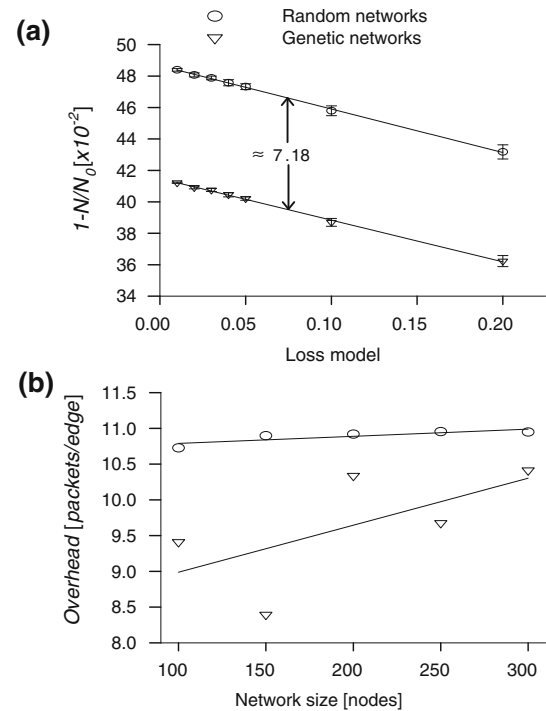

Fig. 12 a Number of packets lost across both random and GRN-derived sensor networks, and **b** average overhead

Moreover, the reduction in the number of packets dropped to the reduction in the number of packets sent were directly correlated. The number of received packets did not vary neither with the inclusion of loss model (1 %) nor with an increase in a loss rate (up to 20 %). However, there is a drop in the number of packets sent due to the inclusion of the loss model. Also, a reduction in the number of packets dropped was observed (as shown in Fig. 12).

6.2 Average overhead is higher in random sensor networks

The average overhead is proportional to the total number of packets sent across the network, and is estimated by calculating the overhead across one edge. The average overhead is measured by an arithmetic average of the total number of packets sent over the ten simulations conducted here, before dividing that value by the total number of edges in the network. Since the number of edges in both GRN—and random-derived sensor networks were equal, the overhead of both GRN—and random-derived networks can be directly compared. As demonstrated by Fig. 12, RWSNs provide a higher average overhead than their GRN-derived model network counterparts. This is can be attributed to the sparse topologies of the GRNs wherein successful packet transmissions are favored through shorter paths to the sink node. The degree distribution of network size 150 is illustrated in Fig. 11.

Table 7 Feedforward Loop Motif Count in GRN-derived sensor networks, RWSNs

Network size	Motif count in GRN-derived sensor networks	Motif count in RWSNs
100	390	138
150	192	80
200	1,424	880
250	330	202
300	2,200	904

6.3 End-to-end delay

The end-to-end delay, defined as the elapsed time for a packet to successfully reach the sink, was measured in all simulations for both GRN—and random-derived sensor networks, and an arithmetic average of these values was used to assess performance in both types of network topologies considered here. Packets dropped by the "loss" models were not considered in the averaging procedure. For the observed network sizes and packet sizes, not much difference was seen in the average end-to-end delays of GRNs and RWSNs. As the GRN and corresponding RWSN have similar number of edges, it appears that the flooding based routing protocol behave similarly on both topologies.

6.4 Observations

We observe that the higher packet receivals in GRN-derived sensor network is due to a significantly higher count of feedforward loop motifs as presented in Table 7. Further analysis on the importance of feedforward loop motifs in providing robustness in GRN-derived sensor networks will be discussed in the context of larger GRN-derived networks in the next section.

7 Experiments on larger GRN derived networks

The GRN-derived networks in each of the previous experiments were generated using GeneNetWeaver which records the GRNs of the following two organisms that are known currently and have been validated: *E. coli* (with 1,500 nodes) and yeast (with 3,000 nodes). Hence, it is not possible to generate larger bio-inspired communication structures using this tool; to cater to these needs, we proposed a directed biological network growing algorithm in (Mayo et al. 2012) that seeks to preserve most of the topological properties of GRNs. In this section, we will present the packet transmission robustness properties of communication structures produced by this algorithm in comparison to RWSNs.
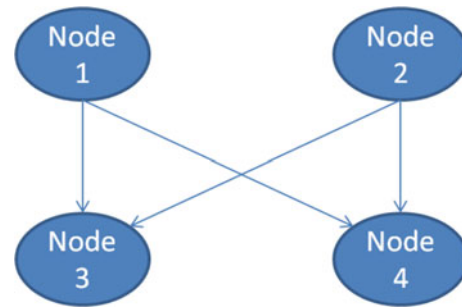

Fig. 13 Bifan motif representation

7.1 Description of a directed biological network (GRN) growing algorithm (Mayo et al. 2012)

An n-node GRN has two distributions describing its total degree: (1) out-degree distribution, $p(K, R, n)$ and (2) in-degree distribution, $q(K, R, n)$ where each node $i = 1, ..., n$ hosts K_i outgoing and R_i incoming links. We developed a preferential attachment (Albert and Barabási 2002) based algorithm for directed GRNs, wherein the network evolution was determined by the following 3 attachment kernels: linear, power-law, and sigmoidal. The GRN is grown by adding nodes one at a time that are attached to the substrate by an average of m directed links to candidate nodes, chosen with equal probability. The probability for an edge from a candidate node to the new one is given by $A(K_i, R_i)$. Similarly, the probability for a link drawn from the new node to a candidate node is $B(K_i, R_i)$. A and B are the out- or in-degrees of the candidate node, and called attachment kernels. The growth algorithm proceeds as follows. Networks were grown stepwise: first, a candidate node is chosen randomly with equiprobability from the existing network of size n. Next, a link directed from the candidate to the new one is drawn if a number (d) randomly selected from (0,1] satisfies $d \leq A(K_i, R_i)$. This is repeated for a link to be drawn from the new node to the candidate, where a new random number satisfies $d \leq B(K_i, R_i)$. The grown networks showed good correspondence with the GRN in *E. coli*.

7.2 Comparing RWSNs and GRNs

Extensive simulations were next performed to establish the importance of GRN-based topologies generated using the new network growing algorithm (Mayo et al. 2012) over RWSNs. NS-2 simulations on 25 networks of each size—100, 150, 200, 250 and 300 have been conducted, however we only report the results for two network sizes 100 and 300 in Figs. 14, 15 as the rest follow the same trend. These results are reported for a packet size of 900 bytes (other packet sizes, mentioned in Sect. 4.2., follow a similar trend). Note that for the RWSNs, we have reported the

Fig. 14 Comparison of best, mean and worst (out of 25) performing RWSNs to GRN—network size 100
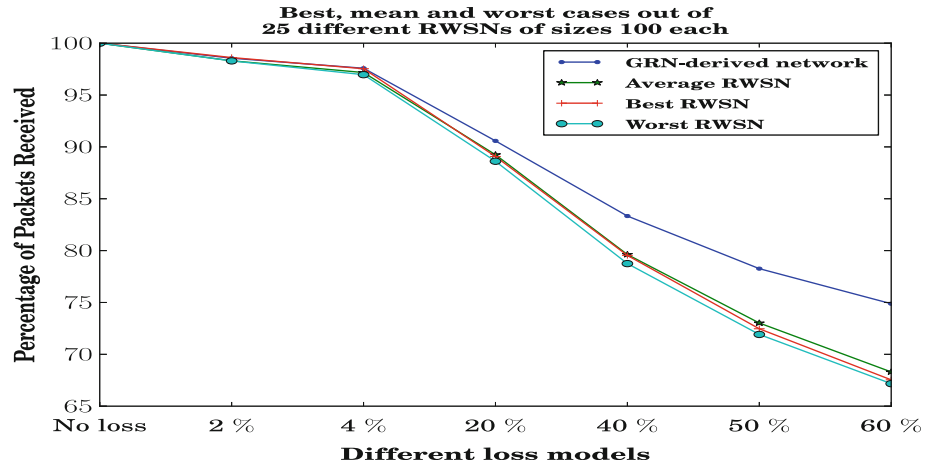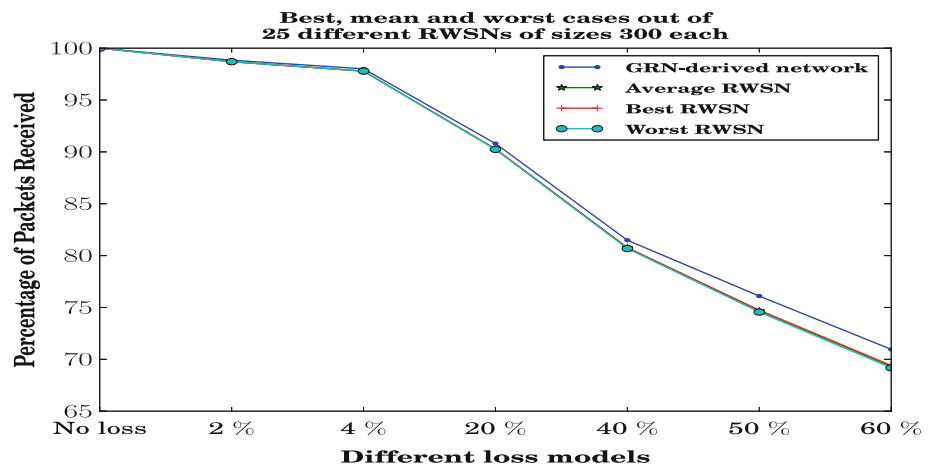

Fig. 15 Comparison of best, mean and worst (out of 25) performing RWSNs to GRN—network size 300

average packet receipt rates for three representative cases having the best, mean and worst network performances (best network is chosen based on the network that has the highest percentage of packets received for loss model 2 %). Also, these results were still generated for smaller sized WSNs primarily to show the robustness features of the network growing algorithm proposed in (Mayo et al. 2012). It can be observed from these figures that these predicted GRNs perform much better than RWSNs for all five different network sizes. We believe that this characteristic can be attributed to the innate structural properties of GRN networks in terms of the number of motifs they contain.

To explore this, we considered the two most important motifs observed in GRNs (Milo et al. 2002) namely, FFLs and bifans. While the importance of FFLs have already been discussed before, bifans were also considered to be important in the context of genomic robustness (Ingram et al. 2006). In fact, while FFLs were responsible for regulating many biological functions, they were found to be less stable (Prill et al. 2005) than bifans (Lipshtat et al. 2007) that signify a 4-node motif structure as shown in

Fig. 13. We counted the number of FFL and Bifan motifs for all the considered networks that is presented in Table 8. The higher motif count in networks generated using the new algorithm is probably why they perform better than randomly generated networks.

To similarly evaluate larger GRN derived networks using the growing algorithm, we considered network sizes of 1,500, 1,750, 2,000, 2,250 and 2,500. We compared the average of all ten networks considered using new algorithm and RWSN approach for network sizes 1,500 and 2,500 in Figs. 16 and 17. Two (for network sizes 1,500 and 2,500) out of five comparisons are illustrated as others follow a similar trend. In general, we observe that the GRN-derived networks still performed better although the improvements in the average packet receipt rates diminished as the network size was increased. We believe that the minimal difference between the performance of new algorithm over RWSN for large networks is not mapping as expected because the new algorithm (although having similar degree distributions) may not exactly replicate the robustness properties of actual GRNs. To observe good performance of GRN-derived topologies for larger networks, better

Table 8 Feedforward loop motif count in RWSNs and new algorithm networks

Network size	FFL count in RWSN	FFL count in new algorithm networks	Bifan count in RWSN	Bifan count in new algorithm networks
1,500	3,933	8,424	7,749	165,848
1,750	3,740	8,514	7,416	166,200
2,000	4,151	8,520	8,259	166,216
2,250	5,666	8,616	11,595	166,548
2,500	6,741	8,580	14,121	166,778

Fig. 16 Comparison of average of ten networks between new algorithm and RWSN—network size 1,500
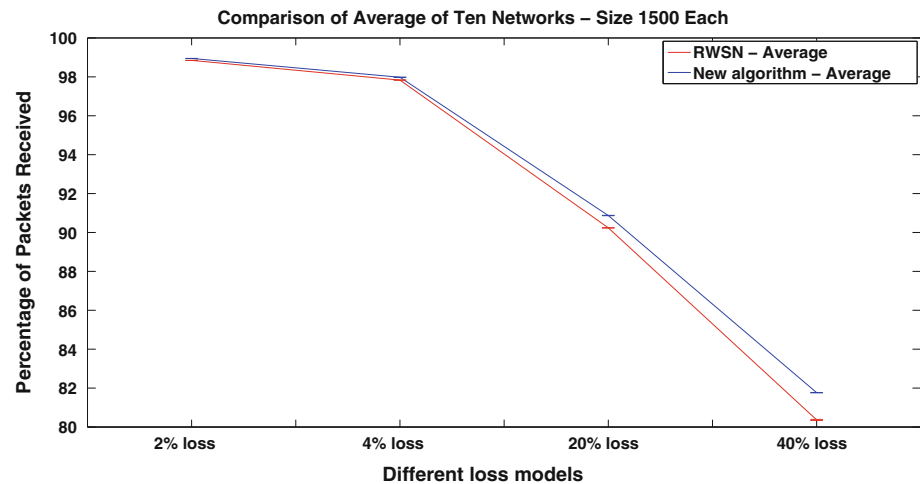
Fig. 17 Comparison of average of ten networks between new algorithm and RWSN—network size 2,500
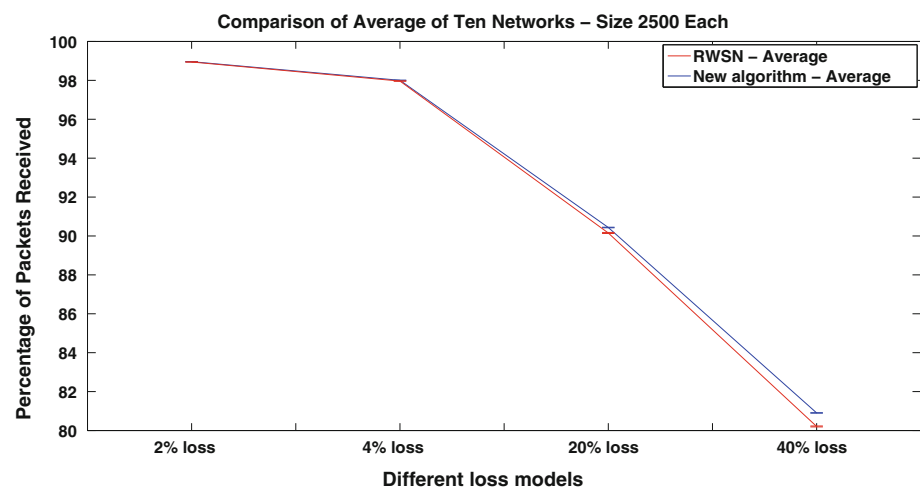
GRN-growing algorithms are needed. Table 8 presents the comparison of respective FFL and Bifan counts for these cases and we still find a higher motif abundance in the predicted GRNs than in the RWSNs. These results point to the fact that motif abundance in itself may not guarantee packet transmission robustness; some other features of GRN topologies may be equally important in imparting robustness and requires further exploration.

7.3 Applications to WSNs

The inherent robustness of such GRN-derived networks opens up many new challenges and application areas for the wireless sensor network research community. Specifically, such GRN-derived networks are sparse and yet possess packet transmission robustness under high channel noise. This should motivate the construction of new routing

protocols in the future wherein GRN-derived networks can be matched to RWSN topologies and only the matched edges can be activated that will both reduce overhead (due to sparseness of GRNs) and increase packet transmission robustness. Multiple graph matchings can be performed to identify robust sections in the RWSN structure wherein fewer edges need to be activated thereby maximizing the coverage area and minimizing the energy consumption overhead. Similarly, communication protocols can be designed by identifying FFL/bifan structures in RWSNs that will ensure packet transmission robustness.

For large-scale WSN deployments, newer network growing algorithms need to be designed that preserve the robustness properties of GRN structures, namely sparseness and motif abundance as observed in GRNs.

8 Conclusion

When the *E. coli* transcriptional network is taken as the result of a sensor "deployment" scheme, transmission scenarios on these networks under variable packet-loss conditions result in smaller packet-loss rates, but also exhibit greater transmission delays than a purely random deployment. On the one hand, it appears that packets more reliably find their way across the network; on the other hand, it takes them longer to do so. This effect arises directly from the topology itself, because the randomly-generated comparison networks were assigned an equal number of links. Scale-free networks are necessarily sparse, possessing few hubs (Genio et al. 2011); so, short direct paths linking opposing sides of the network might also be rare, leading to longer transits.

The transmission time across the network depends on the proper selection of a sink node, of which we proposed four methods: a highest degree based method (HD), an attractor based method (PBN), an FFL-motif based method (MB) and a generalized motif-based method that emphasizes the role a node plays in each FFL motif of the network, termed highest coverage (HC). Interestingly, the HD method predicted nodes as the best candidate to act as the sink in the GRN-derived network. This result, however, is intuitive: the hubs of the GRN-derived sensor networks are strongly connected to the rest of the network, giving them the highest chance of participating in the most sub-networks.

Although we have demonstrated that GRN-derived sensor networks out-perform those of randomly-generated ones with respect to packet-loss rates, but at the expense of longer transmission delays, it remains undetermined how the directionality of GRNs should affect the transmission scenarios in our simulations presented here. Other work (Ghosh et al. 2011) suggests that directionality of the GRN

links have, for example, implications for packet collision events, and future work will incorporate these directional links into the NS-2 simulations.

It was also observed that networks grown through the modified preferential attachment algorithm exhibit a higher number of FFL or bifan motifs that significantly contribute to their packet transmission robustness. However, their performance were comparable to RWSNs as the network size was increased. This reveals the limitations of the preferential attachment based network growing algorithms in generating networks having higher packet transmission robustness and calls for newer algorithms that can more directly reflect the underlying structure of GRNs.

Finally, biological networks, such as the *E. coli* transcriptional network considered here, evolve in response to environmental pressures, yet their topological structures resist homogenization from random mutations of gene bases that occur during every cell division. Transferring these biological principles of network growth into the engineering domain may provide new insights into the design of novel transmission networks that preserve function when exposed to realistic factors such as noise, damage, or targeted attacks.

References

Albert R, Barabási A (2002) Statistical mechanics of complex networks. Rev Mod Phys 74:47–97. doi:10.1103/RevModPhys.74.47

Anastasi G et al (2010) Reliability and energy efficiency in multi-hop IEEE 802.15.4/ZigBee wireless sensor networks. In: Proceedings of the The IEEE symposium on Computers and Communications. ISCC 10. IEEE Computer Society, pp 336–341. doi:10.1109/ISCC.2010.5546804

Couto D et al (2003) A high-throughput path metric for multi-hop wireless routing. In: Proceedings of the 9th annual international conference on Mobile computing and networking. MobiCom 03.ACM, pp 134–146. doi:10.1145/938985.939000

Feng J, Jost J, Qian M (2007) Networks: from biology to theory. Springer, Berlin

Fonseca R et al (2007)Four bit wireless link estimation. In: Proceedings of the 6th workshop on hot topics in networks (HotNets). Atlanta, GA

Foundation P.S. (1991) Core Python Programming. http://www.python.org

Genio D, Gross T, Bassler K (2011) All scale-free networks are sparse. Phys Rev Lett 107(17):178701. doi:10.1103/PhysRevLett.107.178701

Ghosh P et al (2011) Principles of genomic robustness inspire fault-tolerant WSN topologies: a network science based case study. In: 2011 IEEE international conference on pervasive computing and communications workshops (PERCOM Workshops), pp 160–165. doi:0.1109/PERCOMW.2011.57668611

Gnawali O et al (2009) Collection tree protocol. In: Proceedings of the 7th ACM conference on embedded networked sensor systems. Berkeley, CA, pp 1–14

Han B, Leblet J, Simon G (2009) Query range problem in wireless sensor network. Commun Lett IEEE 13(1):55–57. doi:10.1109/LCOMM.2009.081546

Ingram P, Stumpf M, Stark J (2006) Network motifs: structure does not determine function. In: BMC genomics 7(1):108. doi:10.1186/1471-2164-7-108

Kamapantula B et al (2012) Performance of wireless sensor topologies inspired by *E. coli* genetic networks. In: IEEE international conference on pervasive computing and communications workshops, pp 302–307. doi:http:doi.ieeecomputersociety.org/10.1109/PerComW.2012.6197500

Kauffman S (1969) Metabolic stability and epigenesis in randomly constructed genetic nets. J Theor Biol 22(3):437–467

Kim S, Fonseca R, Culler D (2004) Reliable transfer on wireless sensor networks. In: Proc. of IEEE SECON 2004, pp 449–459

Kitano H (2007) Towards a theory of biological robustness. Mol Sys Biol 3:137–144

Li J, Mohapatra P (2007) Analytical modeling and mitigation techniques for the energy hole problem in sensor networks. Pervasive Mob Comput 3(3):233–254. doi:10.1016/j.pmcj.2006.11.001

Lipshtat A et al (2007) Functions of bifans in context of multiple regulatory motifs in signaling networks. In: eprint: arXiv/0711.4937

Mangan S, Alon U (2003) Structure and function of the feed-forward loop network motif. Proc Natl Acad Sci USA 100(21):11980–11985. doi:10.1073/pnas.2133841100

Mayo M et al (2012) Motif participation by genes in *E. coli* transcriptional networks. Front Physiol 3:357. doi:10.3389/fphys.2012.00357

McCanne S, Floyd S (1997) Network simulator. University of California, Berkeley

Milo R et al (2002) Network motifs: simple building blocks of complex networks. Science 298(5594):824–827

Prill R, Iglesias P, Levchenko A (2005) Dynamic properties of network motifs contribute to biological network organization. PLoS Biol 3(11):e343. doi:10.1371/journal.pbio.0030343

Schaffter T, Marbach D, Floreano D (2011) GeneNetWeaver: in silico benchmark generation and performance profiling of network inference methods. Bioinformatics 27(5):2263–2270. doi:10.1093/bioinformatics/btr373

Shmulevich I et al (2002) Probabilistic Boolean networks: a rule-based uncertainty model for gene regulatory networks. Bioinformatics 18(2):261–274. doi:10.1093/bioinformatics/18.2.261

Sun Microsystems I (2009) Link Quality Routing Protocol (LQRP). http://www.sunspotworld.com/docs/Red/javadoc/com/sun/spot/peripheral/radio/mhrp/lqrp/package-summary.html

Tiny OS (2009) The MultiHopLQI protocol. http://www.tinyos.net/tinyos-2.x/tos/lib/net/lqi

Vázquez A et al (2004) The topological relationship between the large-scale attributes and local interaction patterns of complex networks. Proc Natl Acad Sci 101(52):17940–17945. doi:10.1073/pnas.0406024101

Wang C et al (2006) A survey of transport protocols for wireless sensor networks. IEEE Netw 20:34–40

Woo A, Tong T, Culler D (2003) Taming the underlying challenges of reliable multihop routing in sensor networks. In: Proceedings of the 1st international conference on embedded networked sensor systems, pp 14–27